

Operating Characteristics of the Switch Based on a Capillary Discharge with Adjustable Preionization of Cathode Region

P.A. Bokhan, P.P. Gugin, M.A. Lavrukhin, D.E. Zakrevsky

A. V. Rzhanov Institute of Semiconductor Physics SB RAS, Novosibirsk, Russia

The results of studies of a new type of switch [1-3] based on a capillary discharge with a preionization of a cathode region are presented. The cathode region of the switch (fig. 1) consists of two flat rectangular SiC cathodes with a total area of 22 cm² and two grids remote from the cathodes by a distance of 3 mm each and forming a 6 mm region between each other. A capillary of rectangular cross section with dimensions of 10x0.3 mm and a length of 35 mm is located at the side of cathode region. The inner surface of the capillary has a meander shape with a period of 2 mm, which avoids surface breakdowns along the walls of the capillary. Two copper plates connected to the cathodes of the device are attached to the outer surface of the capillary through an additional insulator. Such a configuration allows to reduce the inductance of the switch and has a great influence on providing a large breakdown development time t_d at high pulse repetition frequency (PRF) [2].

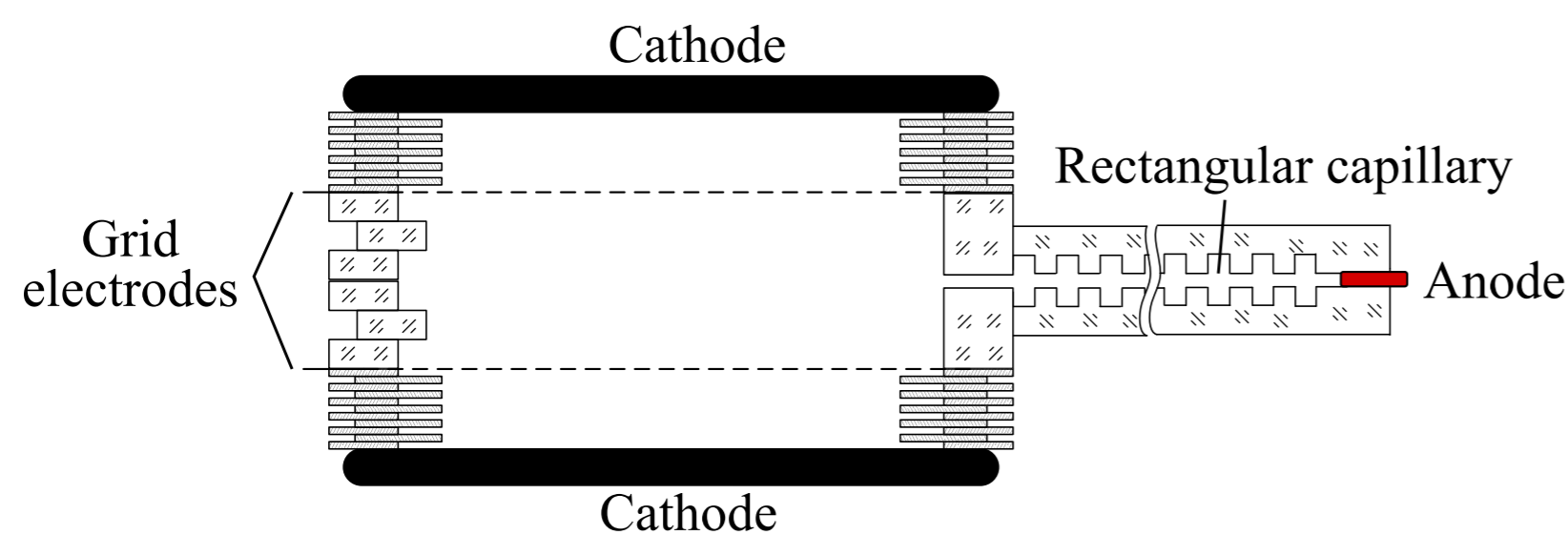


Fig. 1. Drawing of a switch based on a capillary with rectangular cross-section.

The positive voltage pulses from the generator were applied to the anode of the switch, the cathode of the device was grounded (fig. 2a). The charging time of the working capacitance was ~ 200 ns. The value of load resistance R_L varied from 24.5 to 98 Ohm. Parameters were measured in the burst operation mode at a PRF inside the burst f of 5 to 50 kHz. A positive pulse with an amplitude of up to 8 kV was applied between the grids and cathodes to preionize the cathode region 1 μ s before each of the pulses in the burst. Current measurements were carried out using two low-inductance shunts.

In fig. 2a, the oscillograms of the voltage U on the switch and the current through the load I (the sum of the currents through the shunts) are demonstrated. The characteristic voltage switching time is ~ 1.5 ns. Voltage oscillograms for the case of applying the switch with reverse polarity is also presented. In this mode, under similar operating conditions, the starting losses in the switch and the conduction losses during the entire pulse are significantly larger.

At low PRF (units of kHz and less) the starting losses in the switch significantly depend on the degree of prepulse ionization of the cathode region, which, in particular, can be seen in the current oscillograms (Fig. 3a).

The energy deposited into the load in the first 10 ns after the start of switching is taken as a value characterizing the starting losses in the switch. The preionization pulse was applied to the cathode-grid gap 1 μ s before the main pulse, while the oscillograms changed slightly with increasing time up to 5 μ s. The value of the additional capacitance on the grid, C_{pre} , has little effect on the value of the starting losses (Fig. 3b). With an increase in the pre-ionization pulse energy over ~ 10 mJ, the starting losses practically do not change. In addition, the preionization pulse does not significantly affect the total efficiency of energy transfer from the capacitor to the load, except for an increase in starting losses. The breakdown development time in the switch decreases insignificantly (less than 5%) with an increase in the ignition pulse.

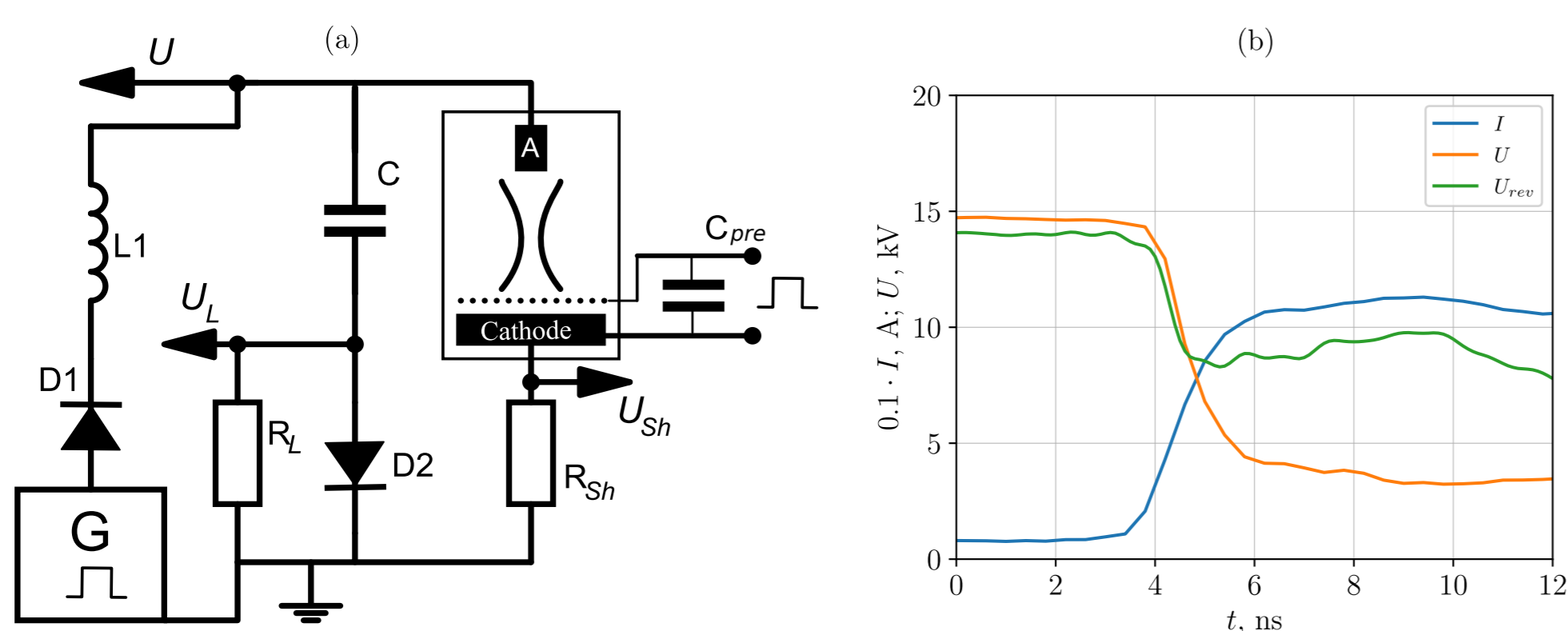


Fig. 2. (a) - electrical circuit for measuring parameters of the switch operation. (b) - Oscillograms of the current I through the load and the voltage U on the switch. U_{rev} is the voltage across the switch when it is connected with reverse polarity (He, $P=10$ Torr, $f=20$ kHz, $R_L=98$ Ohm).

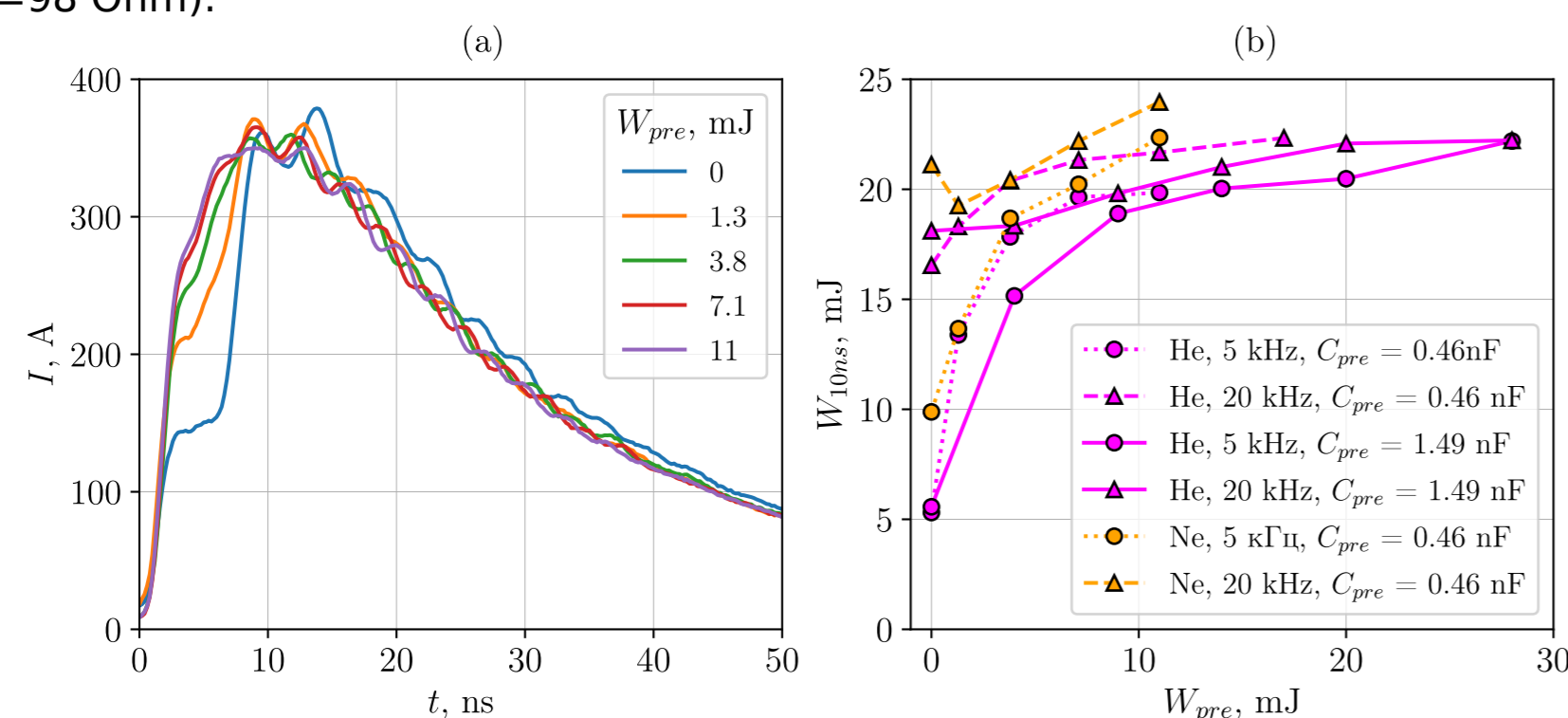


Fig. 3. (a) - oscillograms of current I through the load at different values of the preionization pulse energy of the switch W_{pre} (He, $P=10$ Torr, $U_A=16$ kV, $f=5$ kHz, $R_L=24.5$ Ohm, $C_{pre}=0.46$ nF); (b) - dependences of the energy W_{10ns} deposited into the load during the first 10 ns on W_{pre} ($U_A=16$ kV, $R_L=24.5$ Ohm).

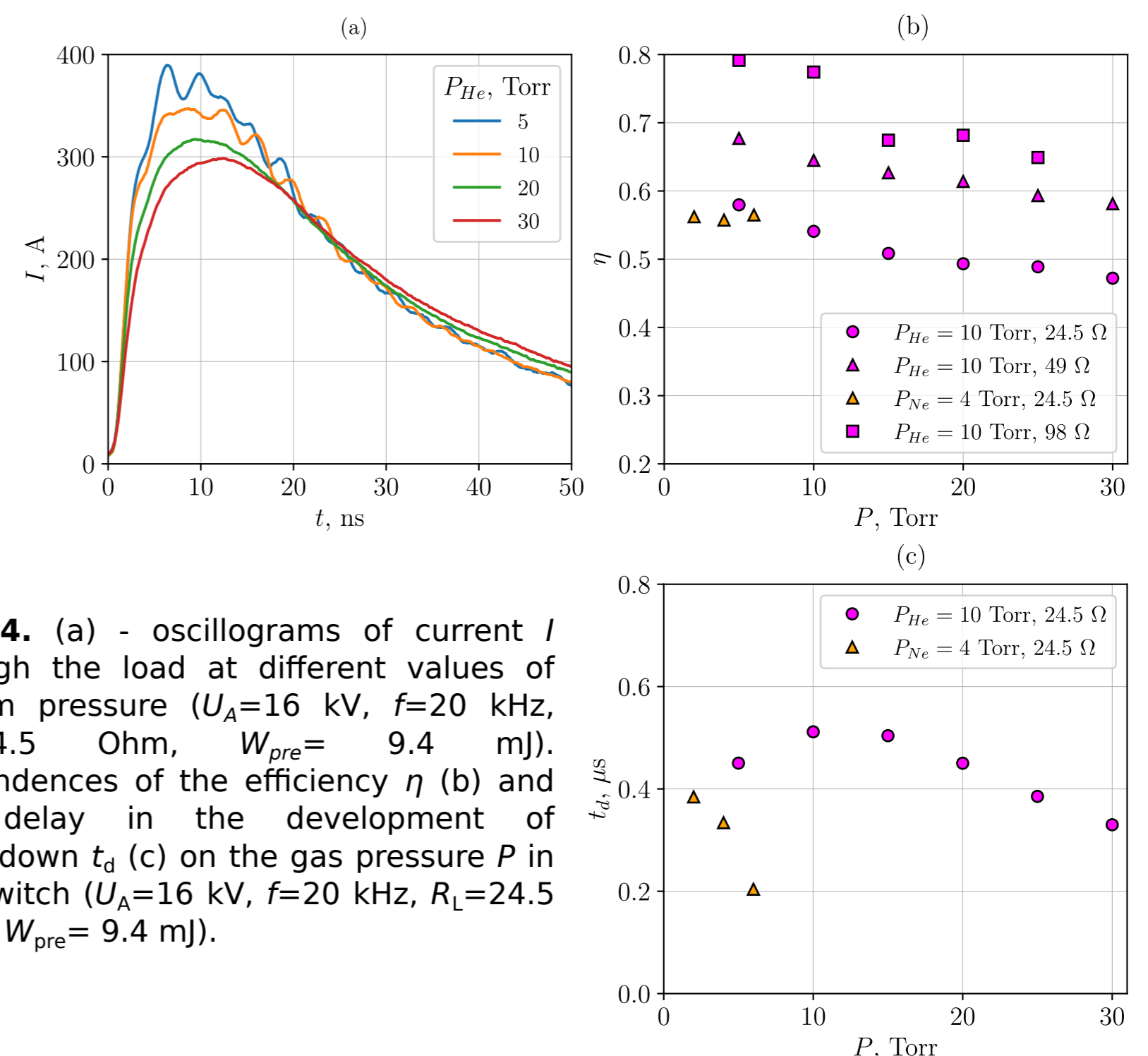


Fig. 4. (a) - oscillograms of current I through the load at different values of helium pressure ($U_A=16$ kV, $f=20$ kHz, $R_L=24.5$ Ohm, $W_{pre}=9.4$ mJ). Dependences of the efficiency η (b) and the delay in the development of breakdown t_d (c) on the gas pressure P in the switch ($U_A=16$ kV, $f=20$ kHz, $R_L=24.5$ Ohm, $W_{pre}=9.4$ mJ).

The conductivity of the switch is significantly influenced by the gas pressure inside it (Fig. 4a,b). On the one hand, with decreasing pressure, the conductivity of the switch and the delay in the development of breakdown (which increases the degree of compression of the leading edge of the voltage pulse) increase, providing favorable conditions for the operation of the switch. But on the other hand, when a certain pressure value is reached (for helium ~ 10 Torr, for neon ~ 3 Torr at $U_A=16$ kV, $W_{pre}=9.4$ mJ), voltage oscillations begin to develop between the switch electrodes, which negatively affects the shape of the signal on the active load (fig. 4a). With an increase in the load, the efficiency of the switch, defined as ratio between the energy dissipated in the load and the energy stored in the capacitor C_0 , increases (Fig. 4b), reaching 0.8 at an amplitude value of the voltage $U_A=16$ kV and a load of 98 Ohm in helium at a pressure of 5 Torr. At similar values of the efficiency in helium, larger values of the delay in the development of breakdown at which the oscillations do not yet occur are attainable than in neon (Fig. 4c).

An increase in the amplitude of the charging voltage U_A leads to an increase in the efficiency of the switch η (Fig. 5a). With a low active resistance - 24.5 Ohm, the efficiency increases from 0.45 to 0.54 with an increase in voltage from 10 to 16 kV in helium. The maximum amplitude value of the voltage in the experiments was 16 kV and was limited by the surface breakdown of the air gap between the conducting plates outside the capillary and its anode. With the organization of additional insulation, it is possible to further increase the operating voltage and, accordingly, the efficiency of the device. The breakdown delay decreases significantly with increasing voltage, reaching ~ 0.5 μ s for 10 Torr helium at 16 kV (Fig. 5b).

The frequency characteristics of the switch are investigated up to $f=50$ kHz. The efficiency of the switch increases slightly with an increase in PRF, which is primarily associated with a decrease in starting losses (Fig. 6a). In helium, after 10 kHz, an insignificant reduction in the breakdown development delay t_d is observed; its value at 10 Torr is ~ 0.5 μ s (Fig. 6b). Thus, up to a PRR of 50 kHz, at a switching time $t_{sw} \sim 1.5$ ns, the compression ratio of the leading edge of the voltage pulse exceeds $S = t_d / t_{sw} = 300$ at $U_A=16$ kV.

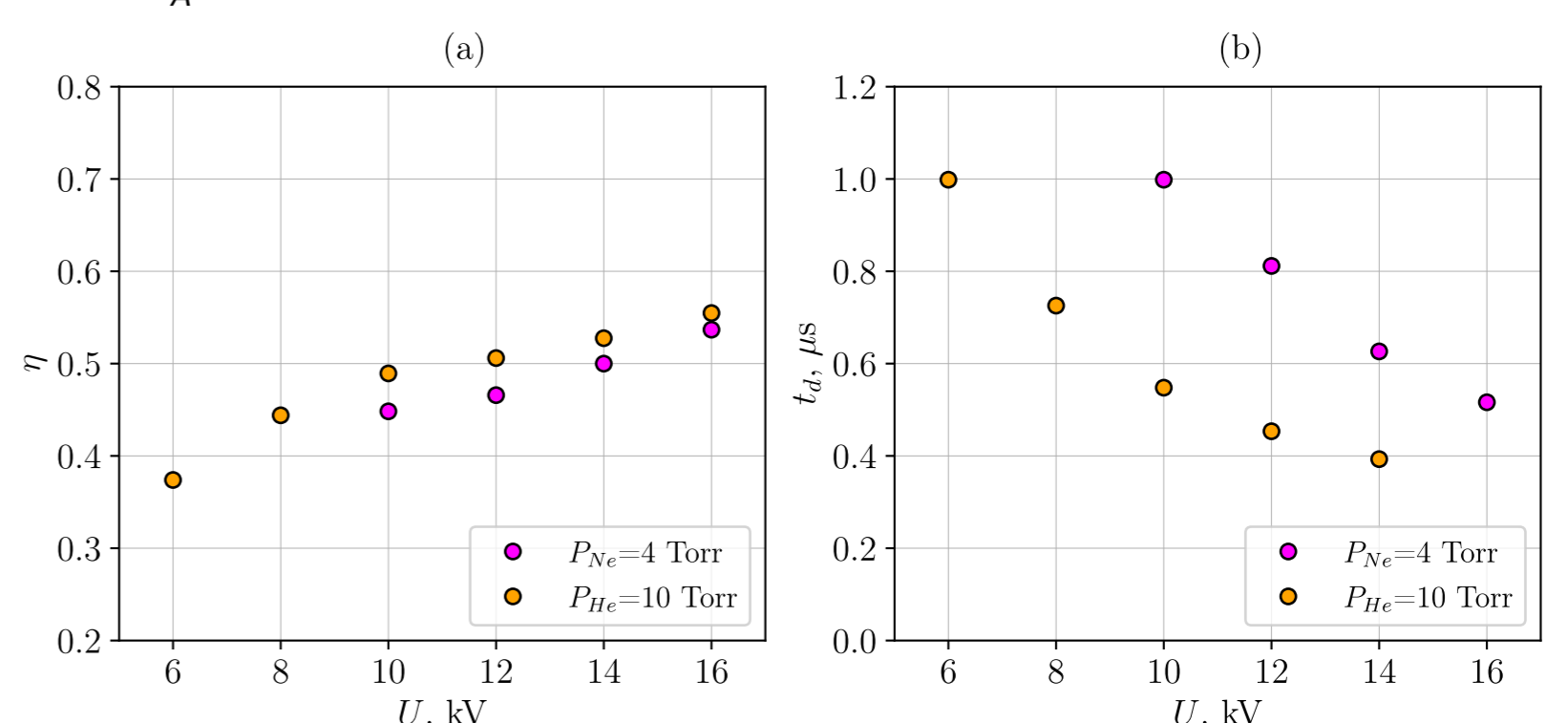


Fig. 5. Dependences of the efficiency η (a), the breakdown development delay t_d , and the switching time t_{sw} (b) on the U_A voltage across the switch ($f=20$ kHz, $R_L=24.5$ Ohm, $C_{pre}=0.46$ nF, $W_{pre}=7.1$ mJ).

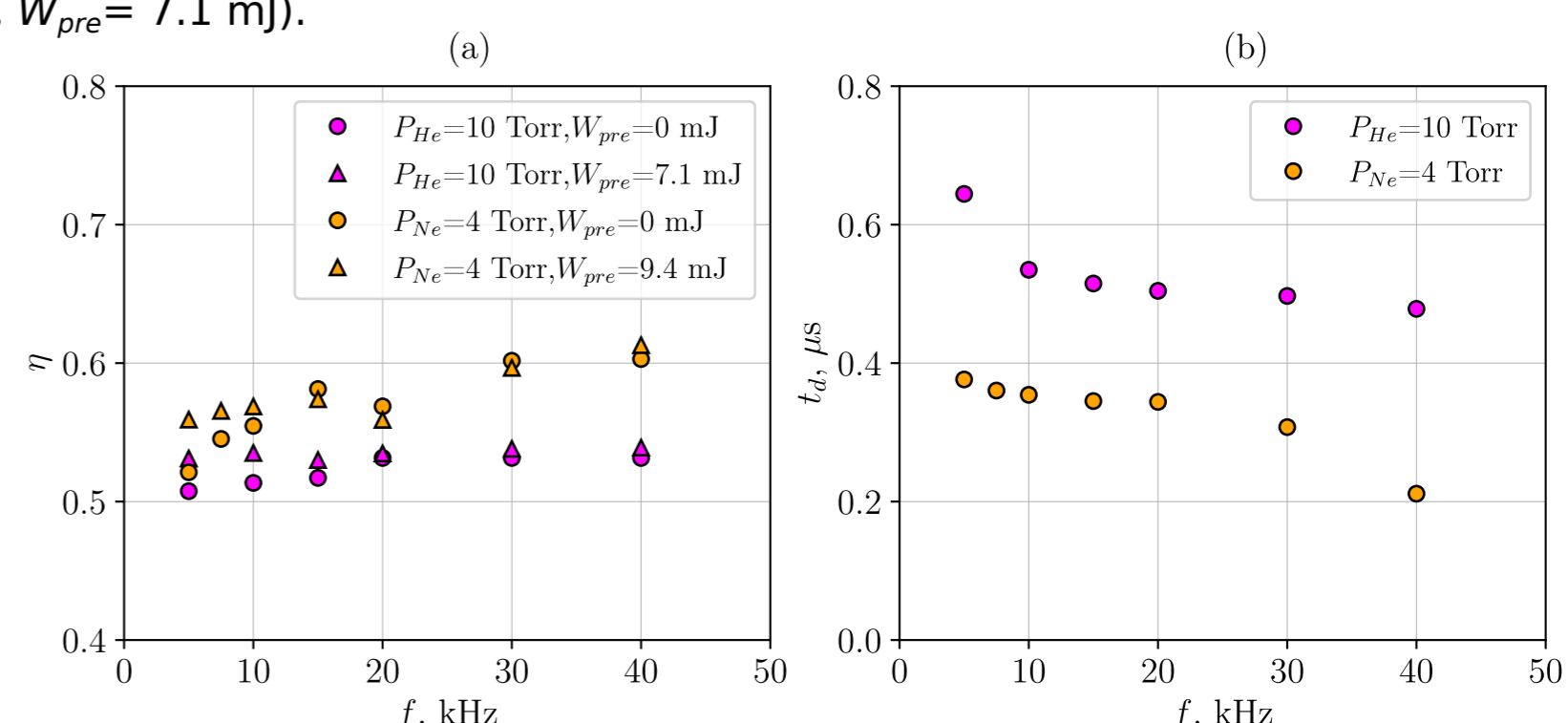


Fig. 6. Dependences of the energy W_{10ns} (a) deposited into the load during the first 10 ns and the breakdown development delay t_d (b) on the PRF f ($U_A=16$ kV, $R_L=24.5$ Ohm, $C_{pre}=0.46$ nF).

[1] P.A. Bokhan, P.P. Gugin, M.A. Lavrukhin, I.V. Schweigert, A.L. Alexandrov, D.E. Zakrevsky, "A high-voltage subnanosecond sharpener based on a combination of 'open' and capillary discharges", J. Phys. D: Appl. Phys., vol. 51, p. 364001, 2018.

[2] P.A. Bokhan, P.P. Gugin, D.E. Zakrevsky, M.A. Lavrukhin, "Frequency Characteristics of a Subnanosecond Plasma Switch", Russian Physics Journal, vol. 62, № 11, p. 2059, 2020.

[3] P.A. Bokhan, E.V. Belskaya, P.P. Gugin, M.A. Lavrukhin, D.E. Zakrevsky and I.V. Schweigert, "Investigation of the characteristics and mechanism of subnanosecond switching of a new type of plasmas switches. II switching devices based on a combination of 'open' and capillary discharges—eptrons", Plasma Sources Science and Technology, vol. 29, № 8, p. 084001, 2020.